INVESTIGATIONS TO REDUCE NOISE AND IMPROVE DATA ACCEPTANCE IN THE GFDL 4-DIMENSIONAL ANALYSIS SYSTEM

K. Puri* and W. Stern
Geophysical Fluid Dynamics Laboratory/NOAA
Princeton University
Princeton, New Jersey 08542
U.S.A.

1. INTRODUCTION

The Geophysical Fluid Dynamics Laboratory (GFDL) and the European Centre for Medium Range Weather Forecasts (ECMWF) were responsible for producing the official level III-B analysis from the FGGE level II-B observations. Rather different approaches to data assimilation were adopted at each center. The GFDL analysis system uses the continuous data insertion approach whereas the ECMWF uses intermittent data assimilation or a forecast-analysis system. Preliminary comparisons of the III-B analyses for the two schemes (Ploshay, et al., 1983; Stern, et al., 1984) indicate that although the analyses show reasonable agreement for the extra-tropical large scales, the GFDL system has shortcomings involving noise and data rejection. Despite the six hourly application of nonlinear normal mode initialization (NMI) to control gravity waves with periods of six hours or less, the insertion of data at each time step excites a significant amount of fast modes. This results in somewhat noisy analyses, and noisy forecasts from these analyses. In addition to the excessive gravity wave noise, there is considerable

*while on leave from Australian Numerical Meteorology Research Centre (ANMRC), Melbourne, Australia.

loss of surface pressure information. A desirable feature of the GFDL analyses when compared to the ECMWF analyses is that it produces a much stronger divergent motion in the tropics.

This study investigates ways to control the amount of fast modes in the GFDL system and methods to reduce the rejection of surface pressure data without altering the tropical characteristics of the system. Section 2 will include brief descriptions of the assimilation and initialization schemes. The experiments will be described in Section 3, some results in Section 4 followed by concluding remarks in Section 5.

2. THE GFDL DATA ASSIMILATION SYSTEM

As described in Stern et al. (1984), the GFDL 4-dimensional data assimilation system consists of three main phases, namely, pre-processing, assimilation and initialization. A schematic overview of the system is shown in Stern et al. (1984), Figure 1. Although this study focuses primarily on assimilation and initialization, certain aspects of the pre-processing stage such as optimum interpolation (OI) have a very important influence on the assimilation process, and a brief description will be included here.

2.1 Pre-Processing

The first part of the pre-processing involves sorting the level II-B data by type, blocking it into six hour intervals and performing quality control checks. Next, OI is used to prepare insertion data at 19 mandatory pressure levels with the model's grid arrangement. The OI is univariate with a vertical range of three mandatory pressure levels and a horizontal influence region of 250 km. Twelve hours of data are processed in two hour blocks via six separate OI analyses. The first guess used for all the OI is the most recent synoptic time analysis available (00Z or 12Z) after it has been initialized. A maximum of eight observations within each grid influence region are used in the OI step, which, in addition to the analysis values, generates weights that are computed on the basis of expected analysis error variance. The weights are further adjusted prior to assimilation of the insertion data in the model (for more details see Stern et. al., 1984).

2.2 Assimilation

The pre-processed insertion data is assimilated into the forecast model by replacing the model solution at each time step by a weighted combination of the OI analysis value, where available, and the model solution at the start of the two hour cycle. The same weighted value is inserted over the two hour period after which the new OI analyses are used for the next two hour period.

The model used in generating the III-B analysis was the GFDL global spectral model rhomboidally truncated at wave number 30 with 18 levels in the vertical (Gordon and Stern, 1982). The so-called E2 physical processes package (Miyakoda and Sirutis, 1977) was used, with the main feature being the Monin-Obukhov formulation in the surface layer. Diurnally varying solar radiation was also included.

2.3 Initialization

As described in Stern et al. (1984), the GFDL operational FGGE system included a Machenhauer (1977) type nonlinear (NL) normal mode initialiation (NMI) with a frequency filter (only modes with periods ≤ 6 hours are adjusted) performed every 6 hours. The use of the frequency filter allowed the strength of the tropical divergent circulation to be retained during initialization. Puri and Bourke (1982) and Puri (1983) have shown that most of the tropical divergent motions are confined to a relative few low frequency gravity modes. The 6-hour cutoff scheme used in the GFDL system, although not the most ideal, does accomplish the essential purpose of controlling much of the gravity wave noise while retaining the tropical divergence. With the nine level model used in this study, only the first four vertical modes were adjusted via three iterations of the nonlinear NMI.

Considerable use has been made of the incremental linear (IL) NMI scheme reported by Puri et al. (1982) and a brief description of the scheme will be given here. The IL scheme essentially subtracts out gravity modes from increments to the model state due to insertion of data. Thus for vertical mode n

$$\Delta y^{I}(n) = \Delta y^{A}(n) - \sum_{sj}^{G}\sum \gamma_{j}^{s}(n)\hat{y}_{j}^{s}(n) \qquad (1)$$

where $\Delta y^{A}(n)$ is the analyzed increment (difference between the OI analysis and the model solution) to the model state, $\Delta y^{I}(n)$ is the linearly initialized increment, $\hat{y}$ is the Hough vector function, γ_{j}^{s} are the expansion coefficients, s is the zonal wave number, and $\sum_{j}^{G}$ denotes a summation over gravity modes only. Thus for vertical mode n the initialization model state is

$$y^{I}(n) = y^{O}(n) + \Delta y^{I}(n) \qquad (2)$$

where $y^{O}(n)$ is the model state before the insertion of data. Since the IL scheme does not directly affect the background model field, it should

Table 1. Model, assimilation and initialization features used in the control and experimental assimilation cycles. M-O = Monin-Obukhov and V. Mode is the vertical mode.

EXPERIMENT	MODEL FEATURES			ASSIMILATION FEATURES	INITIALIZATION	
	Horiz. Res.	# Vert. Levels	Key Physics		NL NMI	IL NMI
CC	R30	9	M-O Surface layer, moist conv. adjust. daily averaged radiation	Stnd. FGGE System	V. Mode 1-4[1] (6 hr. cutoff)	None
EC1	"	"	"	"	V. Mode 1,2[2] (no cutoff) V. Mode 3,4 (6 hr. cutoff)	V. Mode 1-4 (no cutoff)
EC2	"	"	"	"	"	V. Mode 1-4 (6 hr. cutoff)
EC3	"	"	"	EC2 system and Geo. corr., updated insertion	"	"
EC4	"	"	"	EC3 system and Cyber OI	"	"
EC5	"	"	"	EC4 system and 500 km range for PSL	"	"
EC6	"	"	"	EC5 system without Geo. corr.	"	"

[1]Nonlinear NMI performed every 6 hrs. in phase with synoptic times (00Z, 06Z, 12Z, 18Z).
[2]Nonlinear NMI performed at synoptic times and every 6 hrs. in phase with new insertion data times (00Z, 01Z, 07Z, 12Z, 13Z, 19Z).

preserve the meridional circulation built up by the model during data assimilation, although it may not necessarily retain changes in the circulation implied by the data.

3. DESCRIPTION OF EXPERIMENTS

As indicated above, the nine level version of the GFDL spectral model rhomboidally truncated at wave number 30 was used in this study. The E2 physical processes package was used and for computational efficiency the option of diurnally varying solar radiation was not used. All other model parameters were as used in the GFDL FGGE III-B analysis system. Since the OI analyses and the weights for each two-hour block were archived at the 19 mandatory pressure levels during the production stage of the GFDL III-B analyses, it was decided to insert these "data" into the model for this study allowing considerable savings of computer time. From the 19 levels of OI analyses and weights, a subset was selected at 11 pressure levels, and, as in the operational FGGE model, they are interpolated to the sigma levels using cubic splines (in this case to 9 levels). The resulting 9 level "data" were taken to be the truth for the purposes of some of the verification measures used. The period May 25 to May 30, 1979 in the SOP-2 stage of FGGE was used for the main experimental cycles. Some experiments were also carried out using data for the period February 17 to 20, 1979.

Three main 5-day assimilation cycles were carried out with their major features and differences summarized in the top three rows of Table 1. The control experiment (CC) was designed to closely approximate the operational FGGE analysis system. The key change introduced in experimental cycles 1 and 2 (EC1 and EC2) is the addition of IL NMI every time step after data insertion. Hence, EC1 has the same model and assimilation characteristics as CC with IL NMI being performed at each time step after data insertion and the 6 hour period cutoff applied during nonlinear NMI, but only for vertical modes 3 and 4. In EC2 the IL NMI was only performed on gravity modes with periods of 6 hours and less in order to retain more slow gravity modes. The period of 6 hours was taken mainly for consistency with the nonlinear NMI cutoff, which has been shown to be reasonable (Stern, et al., 1984). Cycle CC was repeated with the frequency cutoff applied only to vertical modes 3 and 4. The results were very similar to those from CC.

4. RESULTS

An example of the analyses resulting from each cycle is given in Figure 1 which shows the 500mb height field. The analyses from the three cycles are very similar. However, closer examination indicates that the fields from EC1 and EC2 are smoother than those from CC. The apparent roughness in the CC cycle is in fact an undesirable feature of the GFDL FGGE III-B analyses. It is probably due to an excessive amount of gravity wave noise and also the use of a very small radius of influence in the OI analysis scheme. Hence, the use of the IL initialization has a beneficial effect. Comparison of the mean sea level pressure (MSLP) indicates that EC1 loses more information than CC or EC2 in certain regions, especially in regions of deep low pressure systems. The loss of information in these regions also manifests itself at the upper levels. Comparison of the above analyses with the FGGE III-B analyses produced by the ECMWF indicates a systematic problem with the former in analyzing deep oceanic low pressure systems. The GFDL systems appear to

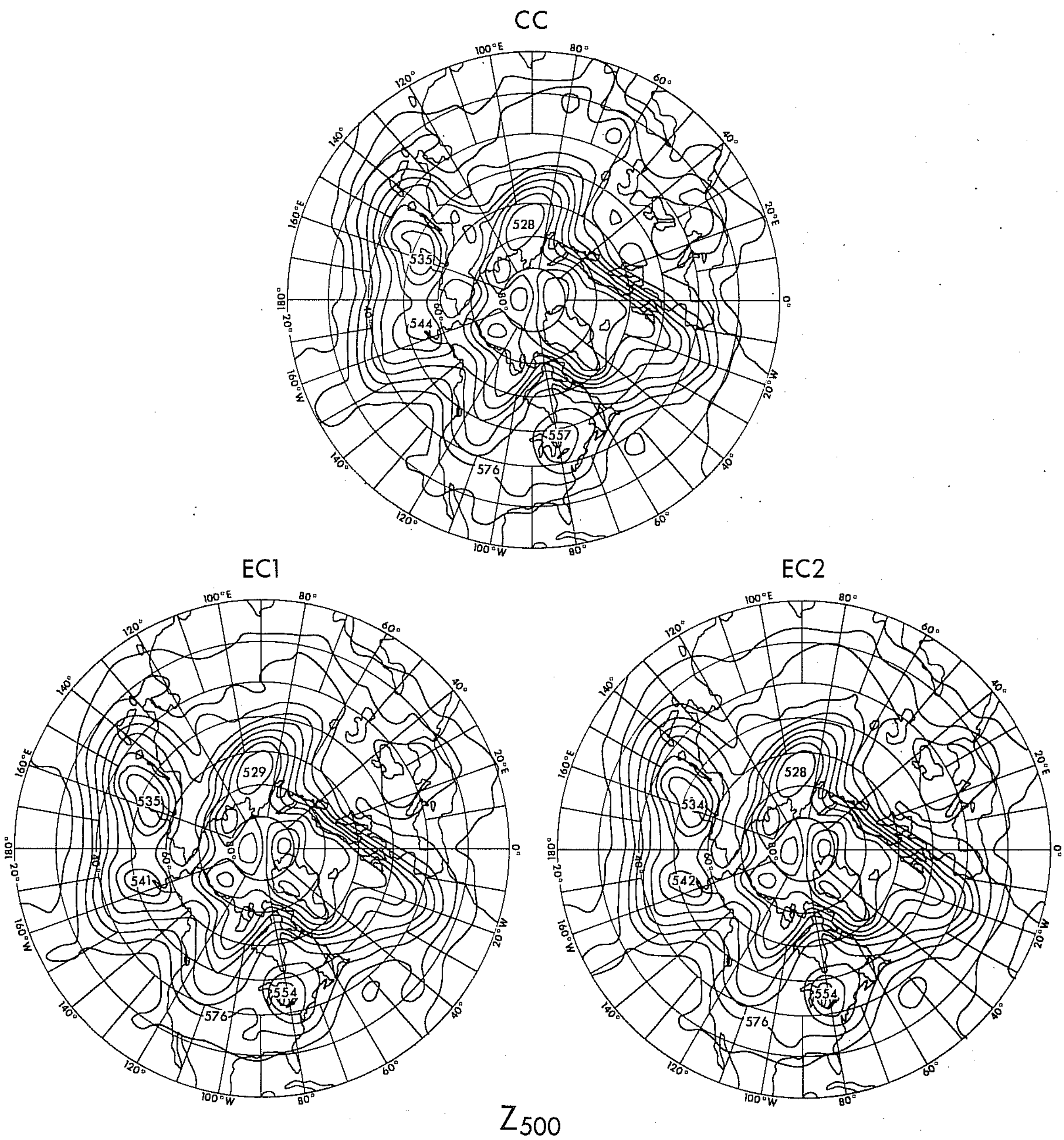

Fig. 1 -- Northern hemispheric maps to 20^{O}N of 500mb height from CC, EC1 and EC2 00Z, May 30, 1979 analyses. Contour interval is 60M.

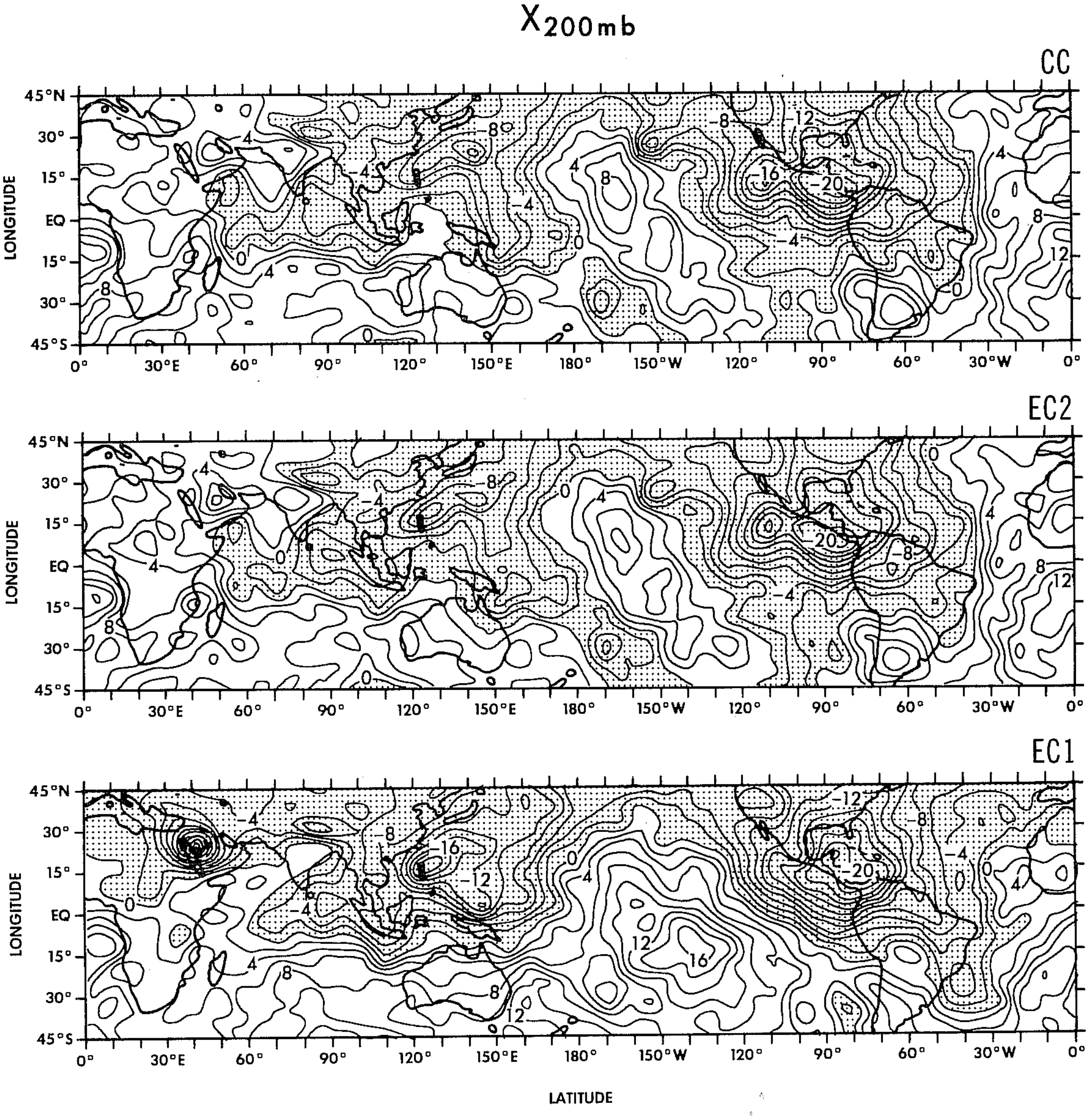

Fig. 2 -- Velocity potential at 200 mb mapped between 45°N and 45°S from CC, EC1 and EC2 00Z May 30, 1979 analyses. The contour interval is 2 M^2 sec^{-1} and negative values are shaded.

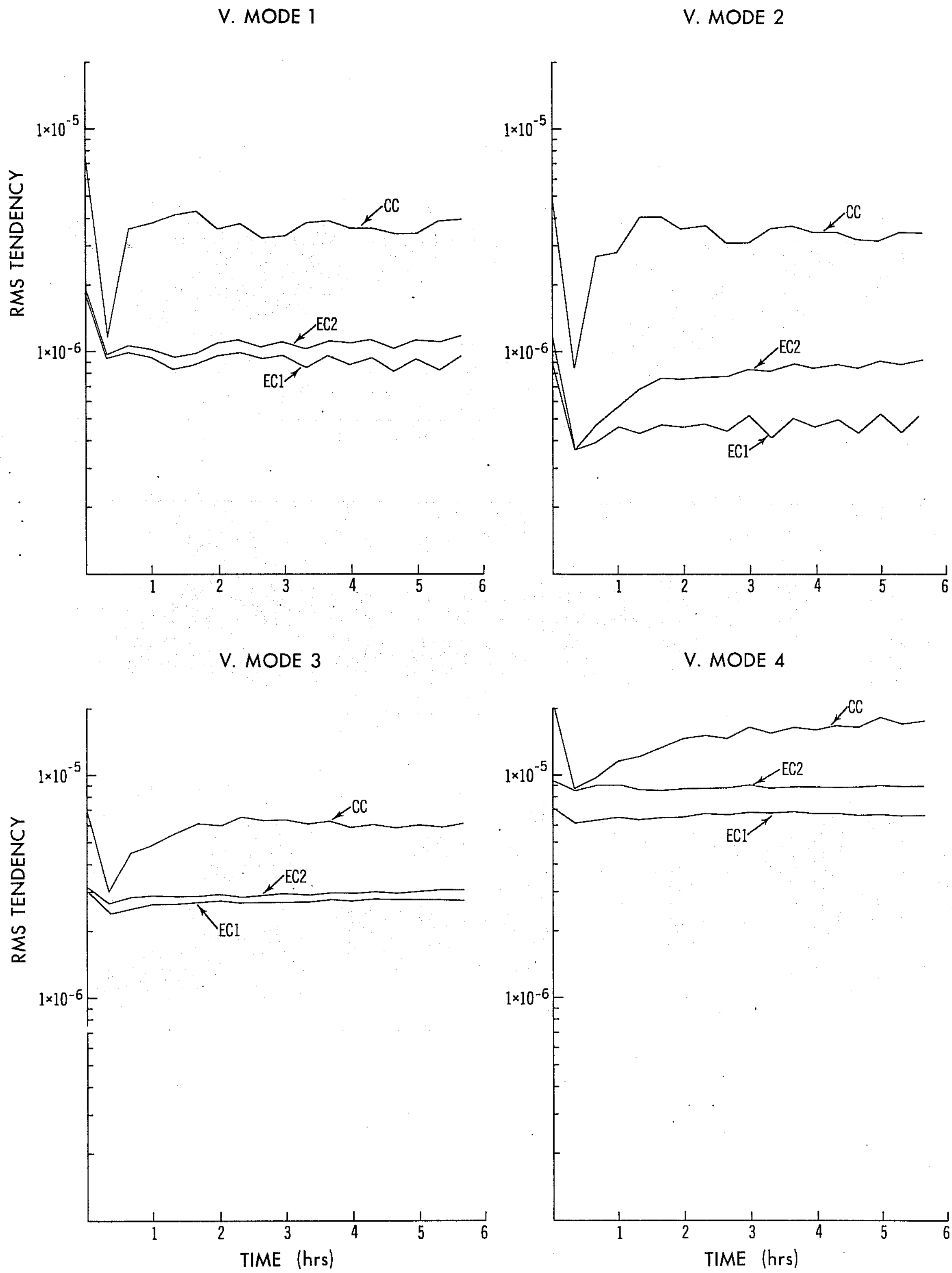

Fig. 3 -- RMS tendency of gravity modes (in sec^{-1}) for each vertical mode (1-4) during 6 hours of assimilation.

consistently underestimate the intensity of these low pressure systems. This aspect will be addressed in more detail later in this report.

The velocity potential field at 200mb resulting from the three cycles after five days of data assimilation is shown in Figure 2. The analyses from the CC and EC2 cycles are very similar. However, significant differences can be seen in the tropics between these two cycles and EC1. This shows that filtering out all gravity modes can lead to the loss of useful information. Hence, removing only the high frequency gravity modes seems more appropriate.

4.1 Noise control

A very important feature of any data assimilation scheme is the level of gravity wave noise inherent in the system. An excessive amount of noise could be detrimental to the resulting analysis via the weighted insertion of a noisy solution. In addition, a high level of fast mode energy is an indication of a lack of dynamical consistency in the model fields and rejection of data, both obviously undesirable. A number of measures were used in this study to indicate the level of gravity wave noise present. Figure 3 shows the root mean square (RMS) tendency of the gravity modes for each vertical mode as a function of time. This quantity provides a direct measure of the level of noise in the model during assimilation. A nonlinear NMI is performed at the initial time which explains the initial drop in the three curves. Subsequent insertion of data leads to an immediate increase in the level of noise in the CC cycle. The level remains at approximately that existing after nonlinear NMI in cycles EC1 and EC2, with EC1 having the lowest rms tendency. These results again indicate the beneficial effect of using IL NMI during continuous assimilation. Another indication of the level of

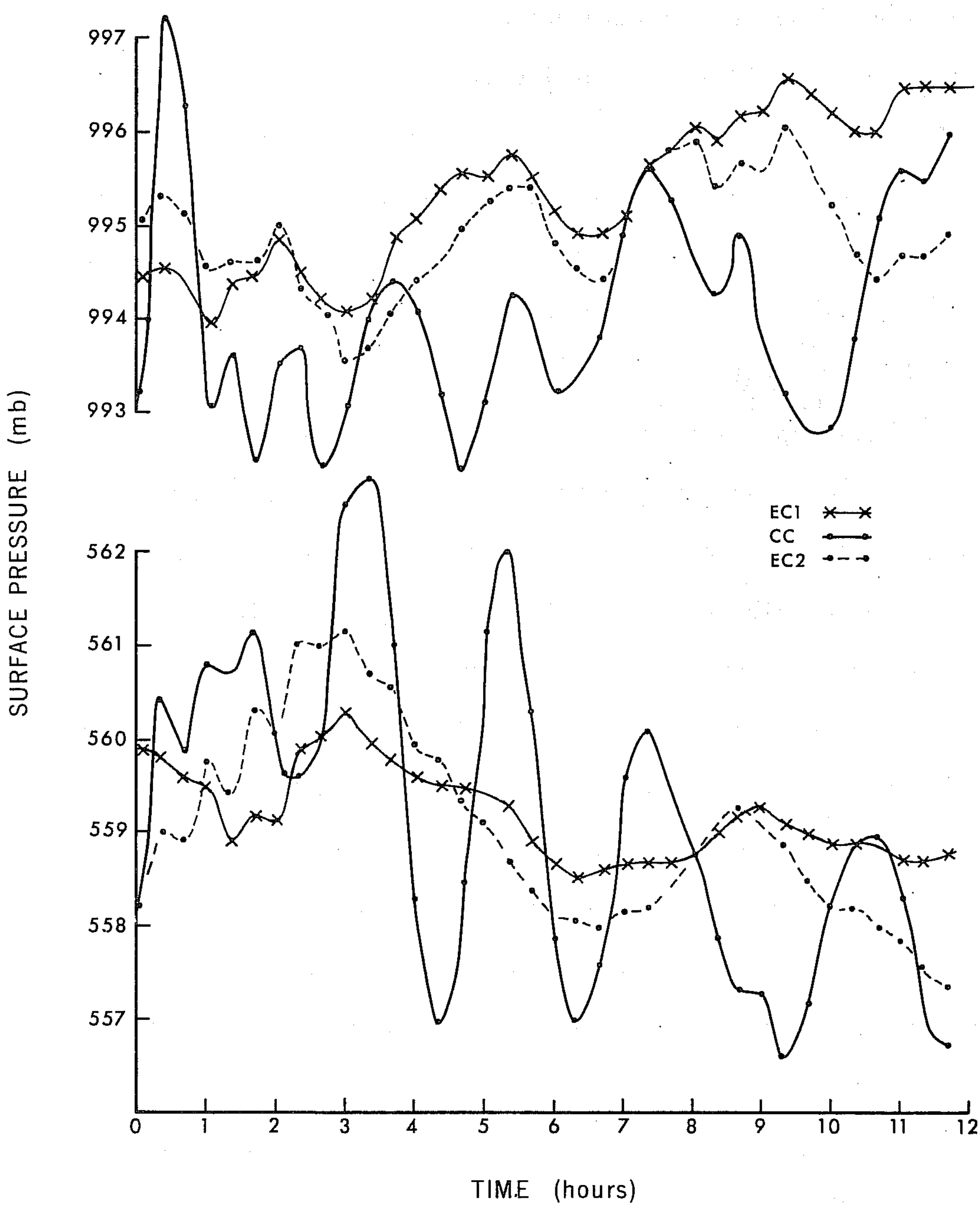

Fig. 4a -- Surface pressure traces, during 12 hour forecasts from CC, EC1 and EC2 00Z May 30, 1979 analyses, at two mid-latitude points.

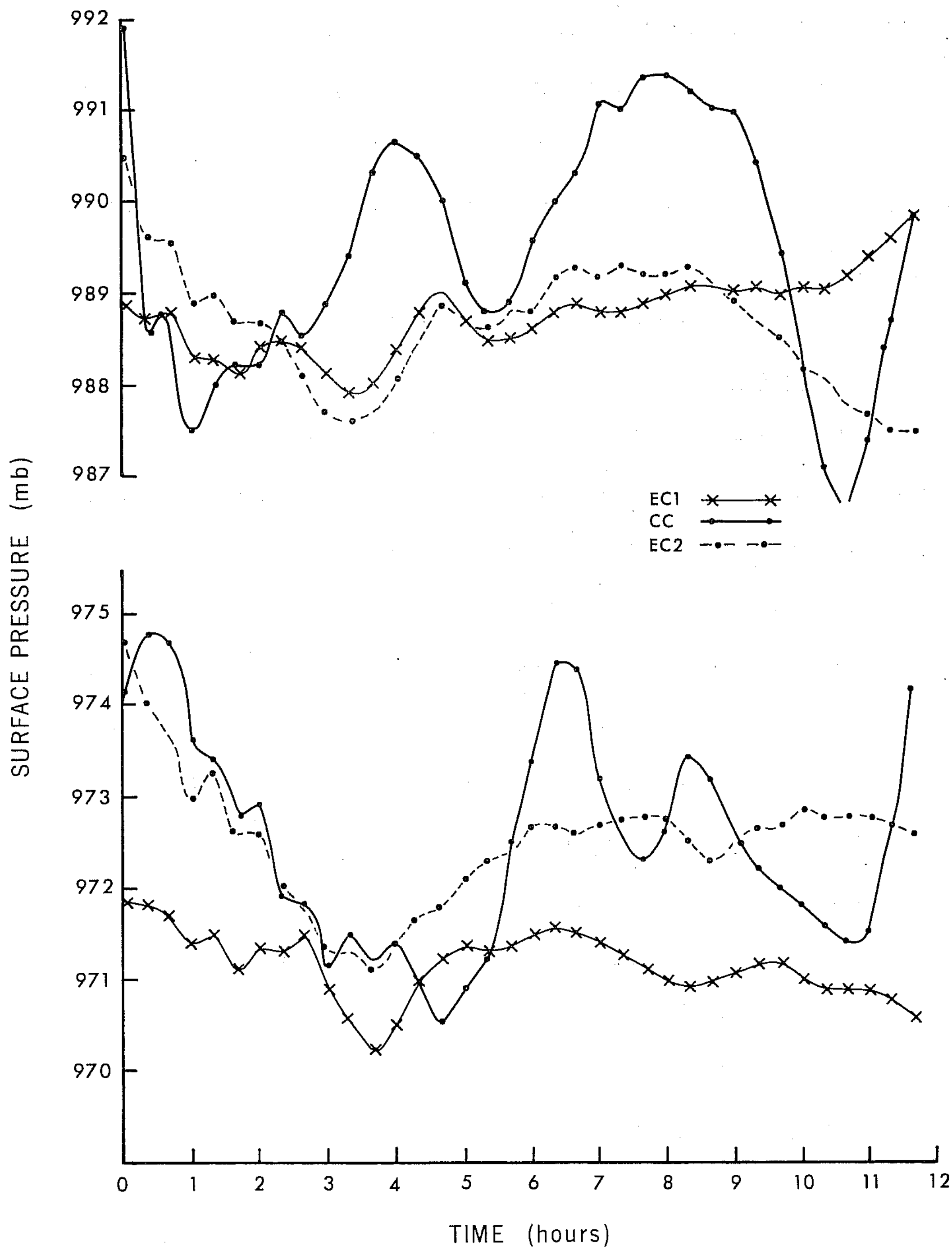

Fig. 4b -- Same as "4a" except at two tropical points.

fast modes in an analysis is the amplitude of high frequency surface pressure oscillations in the initial stages of a forecast. Figures 4a and 4b show surface pressure traces for the various assimilation cycles at two mid-latitude points (top and bottom of Figure 4a) and two tropical points (Figure 4b). It is clear that the high frequency oscillations are greatly reduced for EC1 and EC2 relative to CC. EC1 also appears to be suppressing modes with diurnal frequencies which is especially evident in the tropics, a property that may not be desirable.

4.2 Data acceptance

Data acceptance in the model solution for assimilation systems is obviously important as the solution interacts with observed data to provide a final analysis. Some of the main virtues of continuous assimilation depend on the acceptance of insertion data, for example, the insertion of asynoptic data closer to their observed time involves smaller data windows (i.e. 2 hours vs. 6 hours) so that during any individual time block the analysis may rely more on the model solution. However, if considerable acceptance occurs, the model solution should remain reasonably close to the data.

One measure of data acceptance in the experimental cycles is provided in Figure 5 which plots the global rms difference between the model solution and insertion values (F-I) computed for all points that have insertion data over the 12 hour cycle May 27, 1979 00GMT to 12GMT. As in Stern et al, (1984) for the operational FGGE system, the sharp drops after new data is inserted (new data insertion times are indicated with arrows) shows a degree of acceptance for temperature and wind in all cycles, although, EC1 shows generally greater rms differences, especially for winds, apparently indicating some loss of

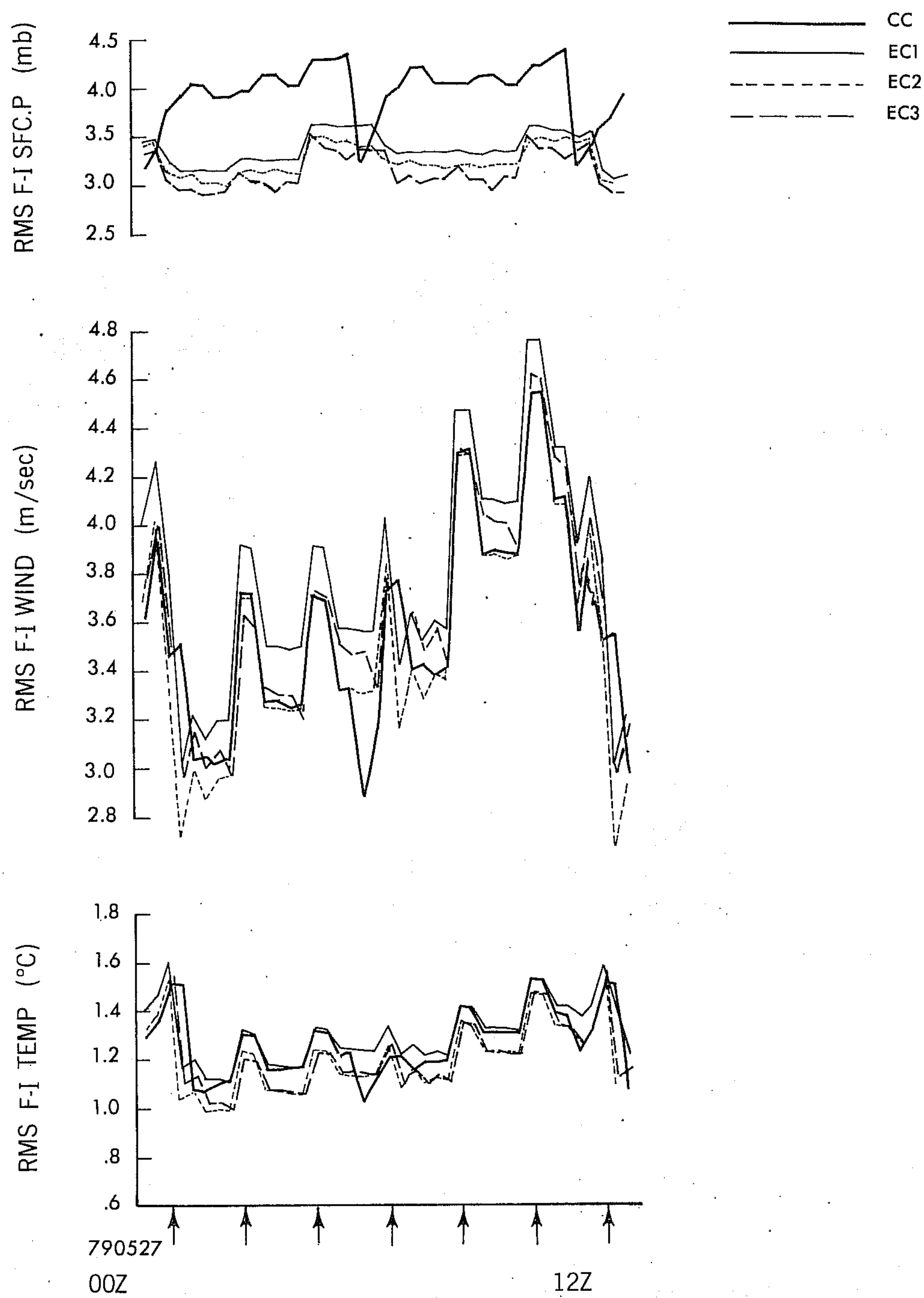

Fig. 5 -- Global rms differences between the model solution and insertion values (F-I) computed for all points that have insertion data. Temperature, winds and surface pressure are plotted for CC, EC1, EC2 and EC3.

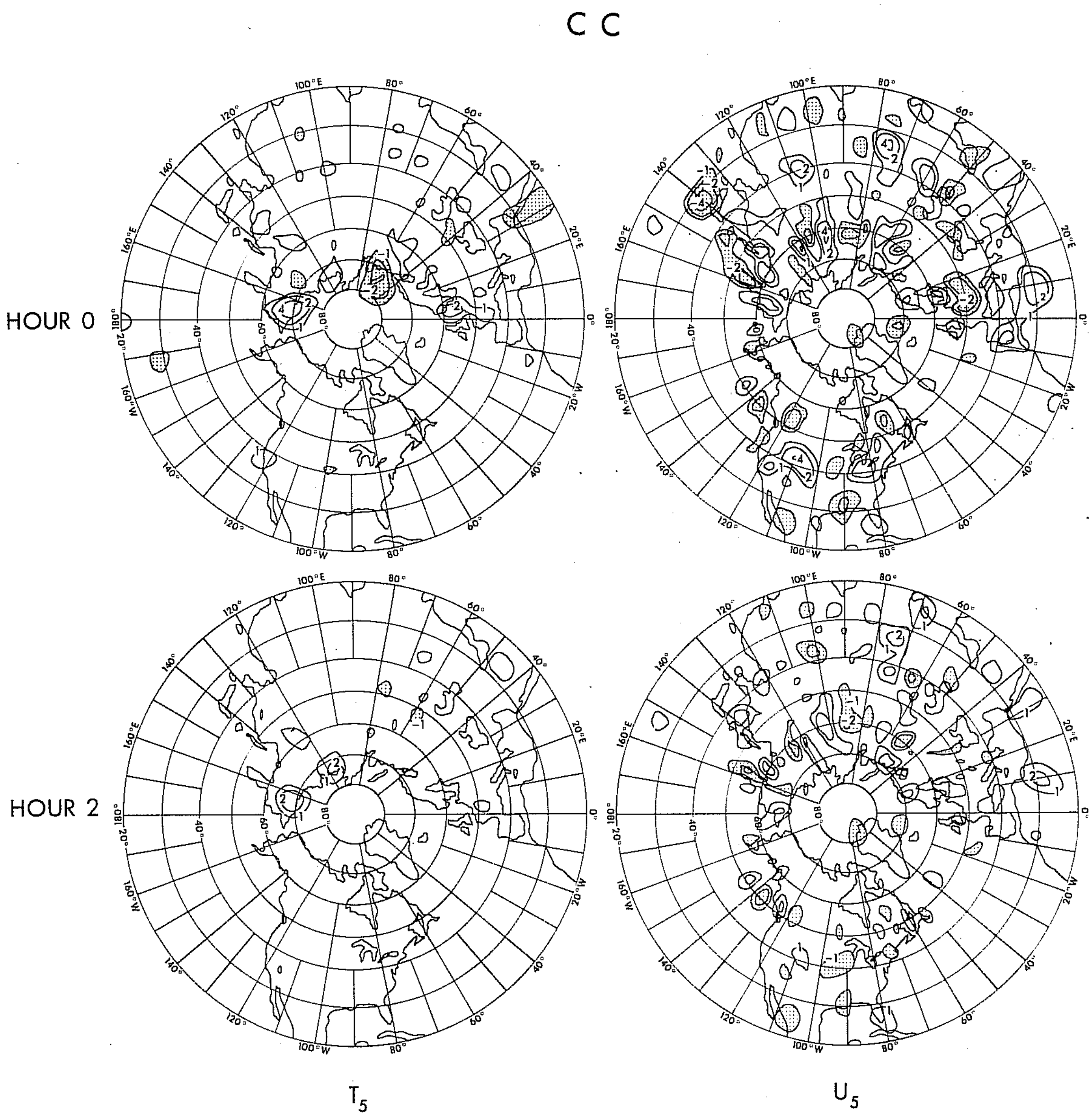

Fig. 6a -- Northern hemispheric maps to 20°N of truncated data increments at sigma level 5 for temperature (left column) and zonal wind (right column) at the beginning (top row) and end (bottom row) of the insertion time block from May 25h01-h03, for CC. Contours = -8, -6, -4, -2, -1, 1, 2, 4, 6, 8; °C, M Sec^{-1} for temperature and zonal wind respectively with negative values shaded.

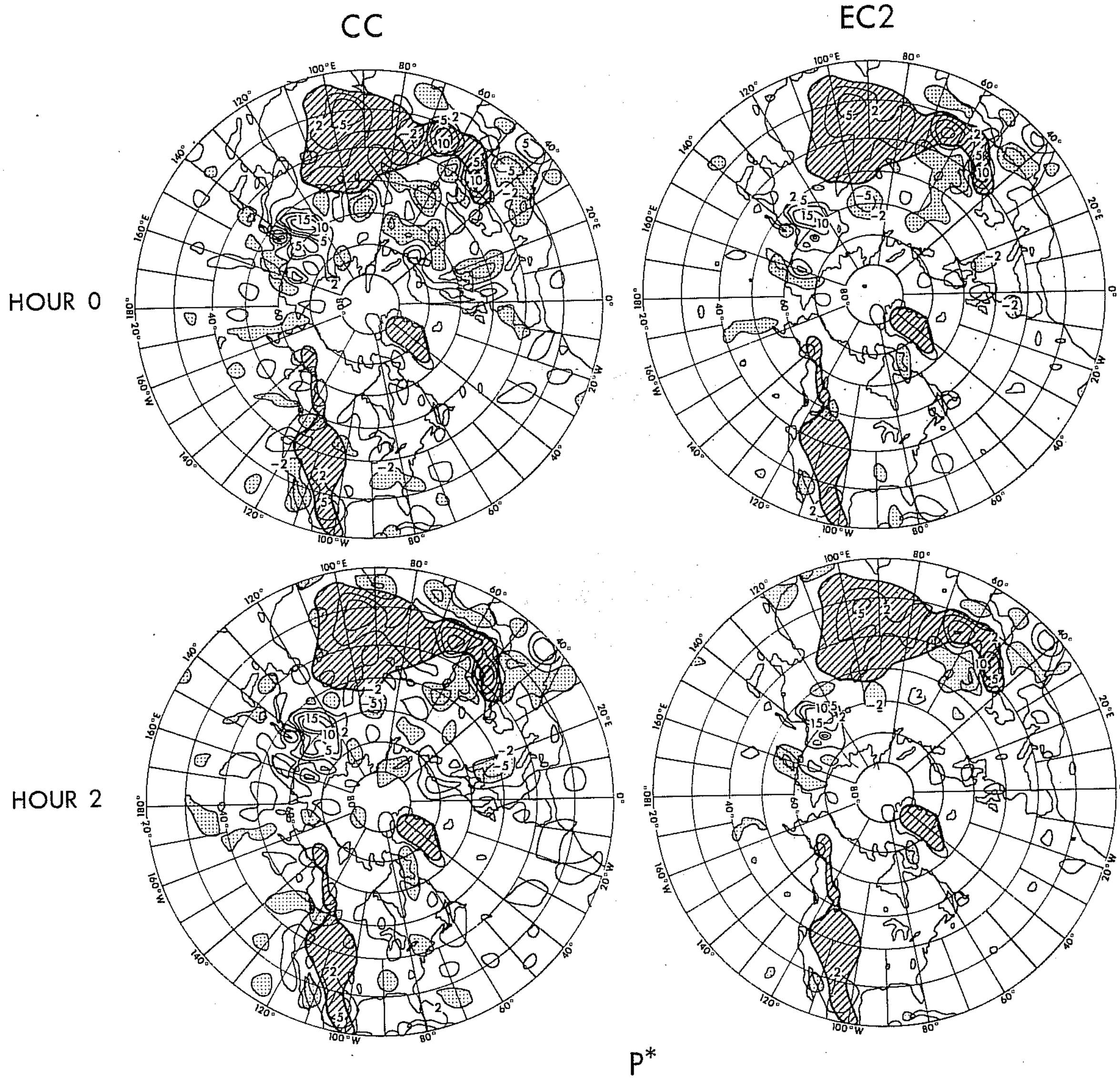

Fig. 6b -- Same as "6a" except surface pressure increments for CC (left) and EC2 (right). Contours (in mb) = -15, -10, -5, -2, 2, 5, 10, 15 with negative values shaded.

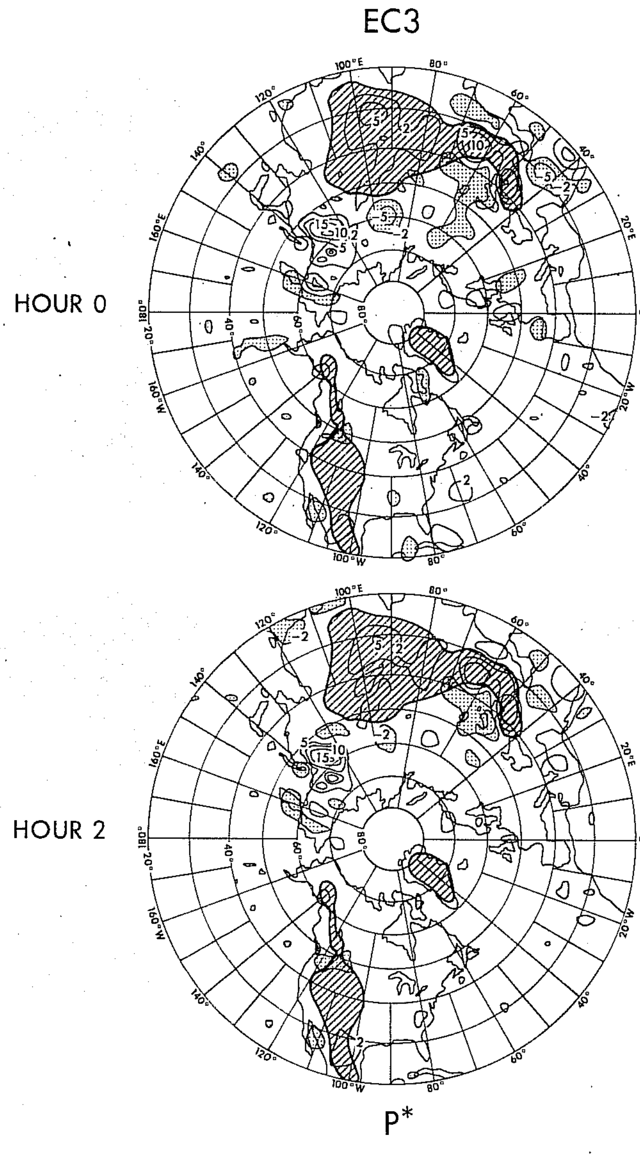

Fig. 6c -- Same as "6b" except for EC3

information contained in the slower gravity modes of the data increments. For surface pressure both EC1 and EC2 show a considerably lower level of rms difference than CC (nearly 1mb), with EC2 about .1mb less than EC1. This is the effect of the significant reduction in the level of fast modes generated during the assimilation by applying the IL NMI which is also confirmed by the sharp reductions in rms difference at the times of nonlinear NMI (see Table 1, footnotes 1 and 2). However, there appears to be virtually no acceptance of the surface pressure by the slow modes in either EC1 or EC2 as the rms difference does not drop after new data is inserted. A fourth curve (EC3) displayed in Figure 5 will be discussed later in this report.

Figures 6a and 6b display insertion data increments (defined as the model solution minus weighted insertion value after truncation) at the beginning and end of a 2-hour insertion time block (May 25 01GMT-03GMT). Figure 6a shows temperature (left column) and zonal wind (right column) data increments at sigma level 5 for the first time step in the 2 hour block (top) and the last time step in the block (bottom), from experiment CC. It is fairly clear that a significant reduction in the magnitude of the large insertion data increments takes place for both temperature and wind, by noting the shrinkage in the size of the area within comparable contour values. This indicates a certain degree of acceptance of the observations by the model solution. In contrast, Figure 6b showing surface pressure data increments from CC (left) and EC2 (right), reaffirms the earlier observation from Figure 5 that essentially no acceptance of surface pressure is taking place. As in Figure 5, generally smaller surface pressure increment values are seen in EC2 but still very little acceptance is taking place.

4.2.1 Geostrophic correction

The tendency for the model solution to reject observed surface pressure is not unexpected considering some earlier findings. Daley and Puri (1980) demonstrated the poor acceptance of mass data inserted in a shallow water model when not accompanied by coincident wind insertion data. More recently, Bourke et al. (1982) investigated this problem in an effort to make better use of the surface pressure data from the southern hemisphere drifing bouys in the ANMRC forecast-analysis data assimilation system. They looked at the projection of southern hemisphere MSLP analysis increments onto the slow and fast manifolds of the assimilating model and found that they projected almost entirely onto the fast modes. Motivated by findings of Hayden (1973) and Kistler and McPherson (1975), which indicated that geostrophic wind corrections derived from mass data could significantly improve the assimilation of mass data, Bourke et al. (1982) incorporated this technique as part of their assimilation system. They showed a substantial improvement in the fit of their initialized MSLP pressure analysis to observations, the hemispheric rms error was reduced by about .5mb which is over 20%. It therefore seems reasonable to apply this procedure to the GFDL assimilation system in an effort to retain more of the surface pressure information. Following Bourke et al. (1982), the geostrophic wind correction may be derived in terms of the spectral model's prognostic variables vorticity and divergence

$$\delta\zeta = \nabla^2 \frac{\delta\Phi}{f} + \nabla\cdot\left[\frac{\delta\Phi}{f^2}\nabla f + \delta\left(\frac{RT}{f}\nabla \ln p_*\right)\right], \qquad (3)$$

$$\delta D = -\hat{k}\cdot\nabla \times \left[\frac{\delta\Phi}{f^2}\nabla f + \delta\left(\frac{RT}{f}\nabla \ln p_*\right)\right]. \tag{4}$$

Where f represents the coriolis parameter, R the gas constant, ζ the vorticity, D the divergence, T the temperature, Φ the geopotential, p_* the surface pressure, ∇ the horizontal Laplacian and δ represents incremental changes to the model solution.

As in the ANMRC system, the geostrophic correction was applied in the troposphere (from σ=.189 to σ=.991), which excludes the top two levels of the nine level model. Because of GFDL's continuous insertion, some modifications to lessen the excessive forcing seemed desirable and even necessary. In the GFDL scheme, geostrophic corrections to the model wind fields are made only where no observations are available; in addition, only 50% of the correction is applied for the first hour of a two hour insertion time block and no corrections are applied during the last hour. The geostrophic correction is also limited to a maximum of zonal wavenumber 15 and was not applied equatorward of 20°. An experimental assimilation cycle (EC3) was devised to test the geostrophic correction scheme, and its key features are summarized in the fourth row of Table 1. In addition to the geostrophic correction, the other modification that distinguishes this cycle from EC2 is allowing the model solution to feedback during the weighted insertion process at every time step rather than only once every 2 hours at the beginning of each new data insertion time. (In Stern et al., 1984, this involves redefining Φ^U_{ijk} and Φ^M_{ijk} in Equation 5, to be the updated model solution and the model solution respectively, at the current time step.) This feedback of the model solution at each time step has been tested without incorporating a geostrophic correction procedure and no real impact was seen. As in the cycles previously described, the FGGE data for May 25 to May 30, 1979 was used for this assimilation experiment.

Returning to the plots of the rms forecast minus insertion differences in Figure 5 for surface pressure, a small reduction in this quantity appears to take place for EC3 after the new data insertion times. The minima for this curve occur after one hour of insertion corresponding to the last geostrophic correction time steps; at this point there is approximately a .25mb reduction relative to EC2. The temperature differences are virtually unaffected but there is some deterioration in the wind differences by about .1msec^{-1}. Both of these effects are more moderate than the experience of Bourke, et al. (1982).

Figure 6c shows hemispheric plots of surface pressure increments at the beginning and end of an insertion data time block for EC3. This corresponds to Figure 6b for CC and EC2. Although there are a few areas where EC3 seems to hint at improved acceptance (i.e. in the vicinity of Norway and Great Britain and also near the Aleutians), generally it appears to be close to EC2. However, a more detailed inspection reveals that surface pressure data increments are reduced to a greater extent in EC3. This can be seen via Table 2, which tabulates surface pressure increment values from the beginning (Hour 0), middle (Hour 1) and end (Hour 2) of the same two hour insertion block used in the Figure 6 charts. This table presents a sample of 17 of the larger values, the same points are shown for both experiments EC2 and EC3. Excluding the very large first increment value, which may be the result of a questionable observation, the mean reduction from the beginning to end of this insertion period is nearly 20% for EC3 and about 9% for EC2. Increments after 1 hour of insertion are also included because this follows the last geostrophic correction in EC3. There is apparently improved acceptance for some points at this time as evidenced by the reduced increment magnitudes in 11 of the 17 cases, but the overall acceptance is about the same.

Comparative test runs of "CC" and "EC3" systems (see Table 1) were also performed using insertion data from February 17 to 20, 1979 during SOP-1. The "EC3" system does exhibit more acceptance of surface pressure than the "CC" system. This may be seen from Table 3 which tabulates surface pressure values during assimilation at 3 gridpoints, aligned north-south near the "Presidents' Day storm", for the last 10 timesteps (19 Feb. 79 21GMT to 20 Feb. 79 00GMT). The timesteps are listed across the top in each section and the three points are indicated along the left from north to south. For each grid point, values from both the "CC" and "EC3" systems are entered showing the model solution, the weighted mix of the OI analysis and the model solution (weighted insertion value) and the truncated weighted insertion value (the analysis available for archiving; what the assimilating model actually sees). Also listed is the OI analysis value before any model-mix, which is constant for each insertion time block (i.e., timesteps 207→212 and 213→218). It is clear that the model solution from the "EC3" system shows more surface pressure acceptance at all grid points, by its closer approach to the truncated insertion values. This even occurs at point 34.7N x 67.5W which has no data available. At the northern point, 39.1N x 67.5W, "EC3" shows only a small improvement (less than 1 mb) in the truncated insertion value despite a large reduction in its gap with the model solution. This is because the OI value gets 100% weight. At the middle grid point the

Table 2. Surface pressure increments (mb) during May 25h01 to h03 insertion time block at selected locations

	N. HEMISPHERE										S. HEMISPHERE						
	55°N – 90°N					20°N – 55°N					55°S – 90°S				20°S – 55°S		
EC2:																	
Hour 0	16.20	-7.63	2.65	3.54	6.95	-2.68	-2.80	-2.57	3.28	2.25	4.83	-2.61	1.62	-2.70	3.89	2.60	3.46
Hour 1	16.07	-6.33	2.23	3.12	5.99	-2.04	-2.00	-2.45	3.32	2.25	4.99	-3.03	1.20	-2.74	3.10	1.45	3.26
Hour 2	16.25	-5.08	2.67	3.32	5.50	-2.04	-2.66	-2.46	2.89	2.33	5.63	-3.19	1.46	-2.84	2.68	1.71	3.58
EC3:																	
Hour 0	16.08	-7.51	2.69	3.67	6.86	-2.82	-2.50	-2.56	3.24	2.13	4.43	-2.17	1.90	-2.72	3.99	2.42	3.35
Hour 1	15.72	-5.84	2.13	3.19	5.14	-2.00	-2.00	-2.35	3.09	1.96	4.36	-2.37	1.37	-2.37	2.59	1.15	3.11
Hour 2	16.07	-4.58	2.61	3.36	5.21	-2.14	-2.18	-2.33	2.71	2.12	4.97	-1.87	1.75	-1.77	1.71	1.39	3.37

Table 3. Evolution of surface pressure (mb) during assimilation at 3 points near the "Presidents' Day Storm" for "CC" and "EC3" type systems from 19 Feb 79 21GMT to 20 Feb 79 00GMT.

Gridpoint = 39.1N x 67.5W

"CC" system-										
Timesteps:	207	208	209	210	211	212	213	214	215	216
Model solution:	1020.6	1019.8	1020.4	1020.6	1020.3	1019.6	1019.5	1017.9	1018.5	1017.6
Weighted insertion value:	1005.4---------------------------->						1003.1----------------->			
Truncated insertion value:	1008.4	1008.5	1008.2	1008.1	1008.3	1008.2	1007.1	1007.2	1006.8	1006.6

"EC3" system-										
Timesteps:	207	208	209	210	211	212	213	214	215	216
Model solution:	1016.6	1015.0	1015.2	1013.7	1015.5	1015.6	1016.0	1013.5	1012.7	1010.2
Weighted insertion value:	1005.4---------------------------->						1003.1----------------->			
Truncated insertion value:	1008.1	1007.9	1007.9	1007.6	1007.8	1007.8	1006.5	1006.2	1006.1	1005.7
OI value:	1005.4---------------------------->						1003.1----------------->			

Gridpoint = 36.9N x 67.5W

"CC" system-										
Timesteps:	207	208	209	210	211	212	213	214	215	216
Model solution:	1009.6	1009.2	1010.9	1010.9	1011.9	1011.2	1010.1	1008.5	1009.3	1008.0
Weighted insertion value:	1005.1---------------------------->						1002.9----------------->			
Truncated insertion value:	1003.3	1003.3	1003.2	1003.1	1003.7	1003.5	1001.5	1001.4	1001.2	1000.9

"EC3" system-										
Timesteps:	207	208	209	210	211	212	213	214	215	216
Model solution:	1009.3	1007.9	1008.0	1006.2	1007.9	1007.7	1008.1	1006.3	1005.1	1002.9
Weighted insertion value:	1005.0	1004.5	1004.5	1003.9	1004.5	1004.4	1002.3	1001.7	1001.3	1000.6
Truncated insertion value:	1004.0	1003.3	1003.4	1002.7	1003.3	1003.2	1001.2	1000.8	1000.3	999.5
OI value:	1002.5---------------------------->						999.6----------------->			

Gridpoint = 34.7N x 67.5W

"CC" system-										
Timesteps:	207	208	209	210	211	212	213	214	215	216
Model solution:	1008.7	1008.5	1009.9	1009.8	1011.1	1010.6	1008.9	1007.7	1008.0	1006.9
Weighted insertion value:	"	"	"	"	"	"	"	"	"	"
Truncated insertion value:	1007.9	1007.8	1008.2	1008.2	1008.8	1008.6	1006.2	1005.7	1005.8	1005.3

"EC3" system-										
Timesteps:	207	208	209	210	211	212	213	214	215	216
Model solution:	1009.8	1009.2	1009.1	1007.5	1008.6	1008.6	1009.1	1008.4	1006.8	1005.1
Weighted insertion value:	"	"	"	"	"	"	"	"	"	"
Truncated insertion value:	1008.4	1008.1	1008.1	1007.3	1007.9	1007.9	1006.3	1006.0	1005.1	1004.2
OI value:	No observations located within influence region									

improved acceptance in the truncated insertion value reaches almost 1.5mb at the end of the period. Complicating the picture a bit is the differences in the truncation effect which should be looked at globally. It should also be noted that in the "EC3" case here, it appears that a significant amount of acceptance of surface pressure is lost when the geostrophic correction forcing is relaxed at the mid-point of the insertion period. This invites investigating additional approaches of applying the geostrophic correction so as to keep more of its beneficial surface pressure retention properties without significant deterioration to the wind analyses.

Despite some encouraging results in the foregoing experiments, it is still evident that considerable rejection of surface pressure information is taking place.

4.2.2 Optimum interpolation range

Another factor to consider is the space scales of the surface pressure increments. (The other variables should also be addressed, but will not be discussed here.) The charts in Figures 6b and 6c give the impression of considerable amplitudes at the small scales. This is confirmed by the solid curve in Figure 7 which shows a power spectrum for a typical incremental surface pressure field produced by the standard FGGE OI scheme. It can be seen that a considerable amount of variance remains in scales greater than zonal wave 15, where it is not reasonable to apply a geostrophic correction. In addition, the flatness of the spectrum implies that a significant portion of the information from the OI analysis may still be beyond the zonal wave 30 truncation limit. In consideration of this foregoing discussion, it seems that more information in larger scales from the OI analysis is needed so that the assimilation model will have a greater chance of accepting the insertion

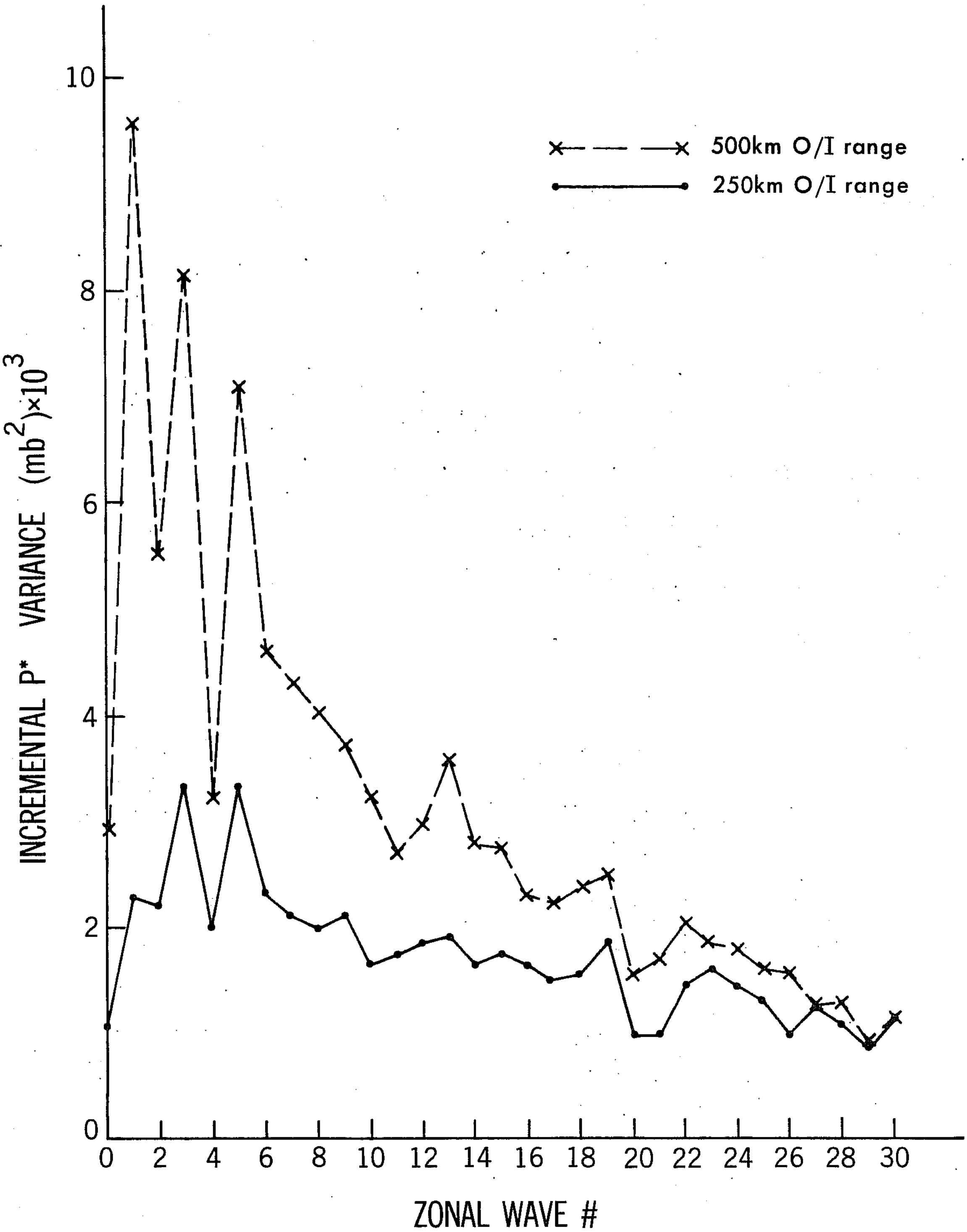

Fig. 7 -- Power spectral analysis of a sample surface pressure insertion field.

data. Hence, the pre-processing of the 79 May 25 00GMT to 30 00GMT FGGE II-B data was repeated using a 500 km radius of influence and allowing up to 12 observations for the sea-level pressure OI analysis (in contrast to a 250 km influence region and a maximum of 8 observations used previously). A substantial increase in the variance of the long waves for incremental surface pressure may be seen in Figure 7 (dashed plot).

In addition to being more appropriate for the assimilating model, the 500 km OI is more consistent with the observational density as evidenced by a much greater percentage of "more informed" OI analysis points. In the 250 km OI out of a total of 4134 MSLP analysis values, approximately 1880 were determined based on only one observation, with about 170 using the maximum of 8 observations. The 500 km OI produces a total of 6254 MSLP analysis values with about 1130 based on one observation, and nearly 1470 using the limit of 12 observations.

Several additional assimilation experiments were set up to test this increased OI range over the period 79 May 25 00GMT to 30 00GMT. The first cycle (EC4) is identical to EC3 except that the OI analysis was regenerated with the "Cyber" system. Up to this point, all experiments used insertion data that resulted from OI analyses generated by the operational FGGE processing system developed with the Texas Instruments ASC computer. When this system was converted for use on the Control Data Cyber 205 computer, small changes were introduced, therefore, it was felt that an exact control case for these additional experiments should be established. An experiment to test geostrophic correction coupled with the 500km OPI (EC5) is identical to EC4, but uses the increased OI range for sea-level pressure. Overviews of these cases are included in Table 1. Five days of data assimilation produce significantly deeper sea-level pressure systems in the generally data sparse regions of the southern hemisphere, where the increased OI range and the geostrophic correction would be expected to have their greatest impact. This is shown in Figure 8 where southern hemisphere MSLP plots of EC5, EC4 (top, left and right, respectively), and the difference EC5 minus EC4 (bottom) are included. It is evident that the low pressure belt surrounding the Antarctic continent is systematically deeper in EC5 relative to EC4. In an effort to ascertain the effect of the increased OI range, exclusive of the geostrophic correction, a final experiment (EC6) was performed identical to EC5 but with no geostrophic correction (see Table 1). The fit of the assimilation model solution to the untruncated surface pressure insertion values (as in Figure 5) provides a measure of the amount of information that is lost. This quantity is displayed in Figure 9 for EC4, EC5 and EC6. It appears that over half of the reduction in the rms difference (about .3mb) is due to the larger OI influence region. By analyzing more information into the larger scales there will be less lost due to truncation. In addition, there may be some increased acceptance by the model solution. As in EC3, the geostrophic correction technique provides an additional increased acceptance of about .25mb.

5. CONCLUDING REMARKS

Progress in overcoming two major shortcomings, a high level of noise and poor acceptance of surface pressure data in GFDL's continuous data assimilation system has been demonstrated.

An incremental linear initialization has been successfully incorporated within the continuous assimilation framework and is quite effective in significantly reducing the amount of noise (i.e. level of

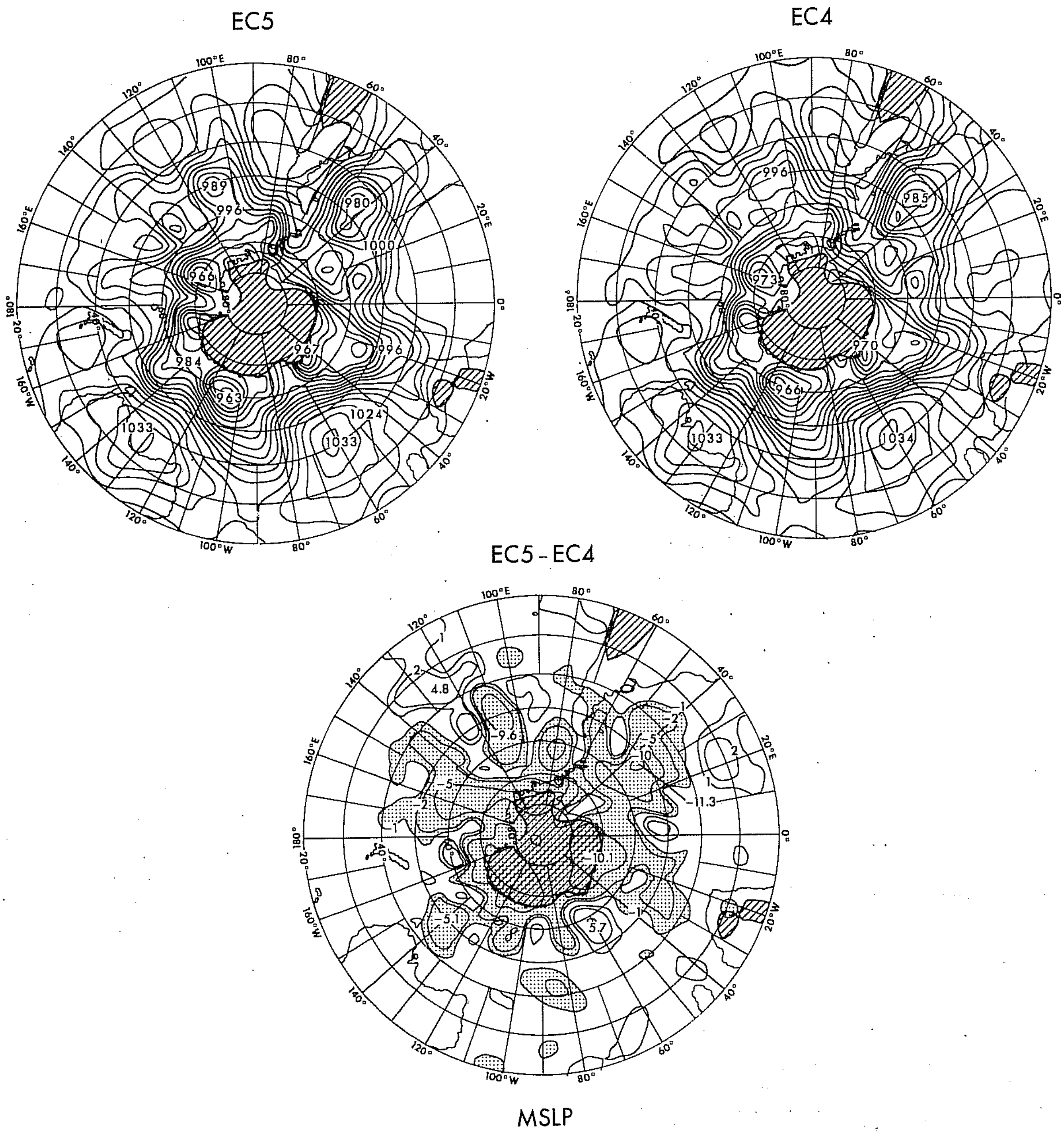

Fig. 8 -- Southern hemispheric maps to 20°S of MSLP for (left to right) EC5, EC4 and the difference EC5 minus EC4. Contour interval is 4mb for EC5 and EC4 maps, and (in mb) -10, -5, -2, -1, 1, 2, 5, 10 for the difference map with negative values shaded.

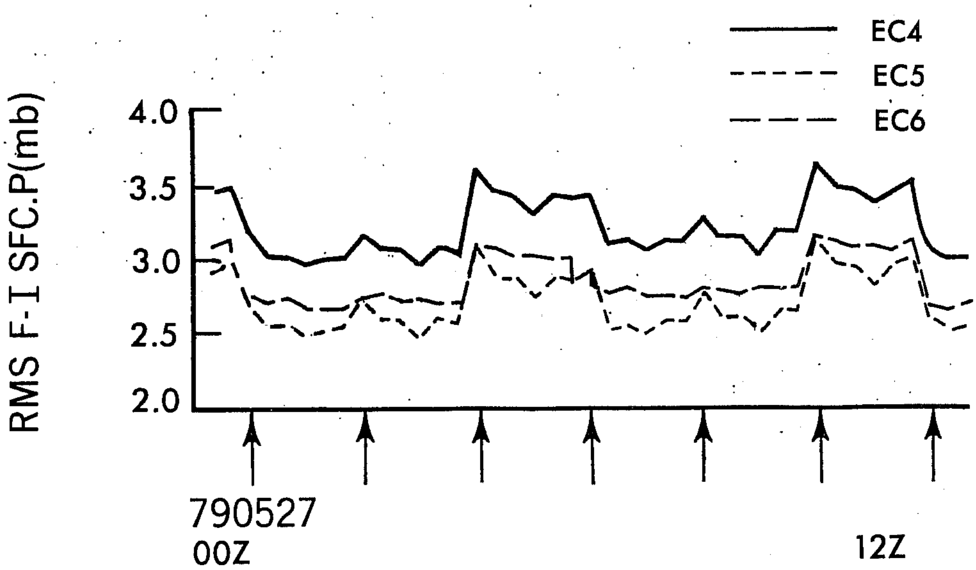

Fig. 9 -- Same as "5" except surface pressure only for EC4, EC5 and EC6.

fast modes) and producing analyses that are better balanced. Furthermore, when the IL NMI is applied selectively (to the higher frequency gravity modes only) the strength of the tropical divergence is retained with very little loss in noise control.

In contrast to reducing the level of fast modes, which is accomplished almost exclusively through one phase of the system (i.e. initialization), improving acceptance of surface pressure appears to involve more of an interaction between the various aspects of the 4-dimensional assimilation system. During assimilation, a geostrophic correction to model winds based on surface pressure and temperature increments shows some improvement in the acceptance of surface pressure with only a small deterioration in the fit of the wind analyses; the IL NMI improves the fit between the model solution and insertion data by keeping the solution close to the slow manifold; and increasing the OI influence region appears to provide for a greater consistency between the model's resolution, the OI analysis and observational data.

In some sense the GFDL system has begun to incorporate the concept of unified analysis-initialization (Williamson and Daley, 1983) at least to the extent of providing for more coupling between the various phases. The IL NMI along with the geostrophic correction should serve to produce more balanced incremental changes to the assimilation model solution. This solution should then help refine the OI analysis by being allowed to feedback during weighted insertion.

Further investigations regarding the OI radius of influence (as well as shortening the cycle to allow for a more current first guess) seem warranted.

6. ACKNOWLEDGMENTS

We are grateful to Dr. K. Miyakoda and Mr. J. Ploshay for their valuable input. Thanks go to the GFDL drafting group and photographer John Conners for their help with the figures and also to Marlene Stern for word processing and editing this paper.

7. REFERENCES

Bourke, W., K. Puri, R. Seaman, B. Mc Avaney and J. LeMarshall, 1982: ANMRC data assimilation for the southern hemisphere. Mon. Wea. Rev., 110, 1749-71.

Daley, R. and K. Puri, 1980: Four-dimensional data assimilation and the slow manifold. Mon. Wea. Rev., 108, 85-99.

Gordon, C.T. and W.F. Stern, 1982: A description of the GFDL global spectral model. Mon. Wea. Rev., 110, 625-644.

Hayden, C., 1973: Experiments in the four-dimensional assimilation of Nimbus SIRS data. J. Appl. Meteor., 12, 425-435.

Kistler, R.E. and R.D. McPherson, 1975: On the use of a local wind correction technique in four-dimensional data assimilation. Mon. Wea. Rev., 103, 431-444.

Machenhauer, B., 1977: On the dynamics of gravity oscillations in a shallow water model with application to normal mode initialization. Beitrage Zur Physik der Atmosphare, 50, 253-271.

Miyakoda, K. and J. Sirutis, 1977: Comparative integrations of global models with various parameterized processes of subgrid scale vertical transports: Description of the parameterizations. Contrib. Atmos. Phys., 50, 445-487.

Ploshay, J.J., R.K. White and K. Miyakoda, 1983: FGGE Level III-B daily global analyses, Part I to IV. NOAA Data Reports GFDL-1, GFDL-2, GFDL-3 and GFDL-4.

Puri, K. and W. Bourke, 1982: A scheme to retain the Hadley circulation during nonlinear normal model initialization. Mon. Wea. Rev., 110, 327-335.

Puri, K., W. Bourke, and R. Seaman, 1982: Incremental linear normal mode initialisation in four dimensional assimilation. Mon. Wea. Rev., 110, 1773-85.

Puri, K., 1983: The relationship between convective adjustment, Hadley circulation and normal modes of the ANMRC spectral model. Mon. Wea. Rev., 111, 23-33.

Stern, W.F., J.J. Ploshay, and K. Miyakoda, 1984: Continuous data assimilation of GFDL during FGGE. (Submitted to ECMWF 1984 Seminar Proceedings).

Williamson, D. and R. Daley, 1983: A unified analysis-initialization technique. Mon. Wea. Rev., 111, 1517-1536.